

pubs.acs.org/Macromolecules Article

Oxidative Polymer Degradation via Cope Elimination

Jared I. Bowman, James B. Young, Victoria L. Thompson, Kevin A. Stewart, Lily E. Diodati, Kaden C. Stevens, Cabell B. Eades, and Brent S. Sumerlin*

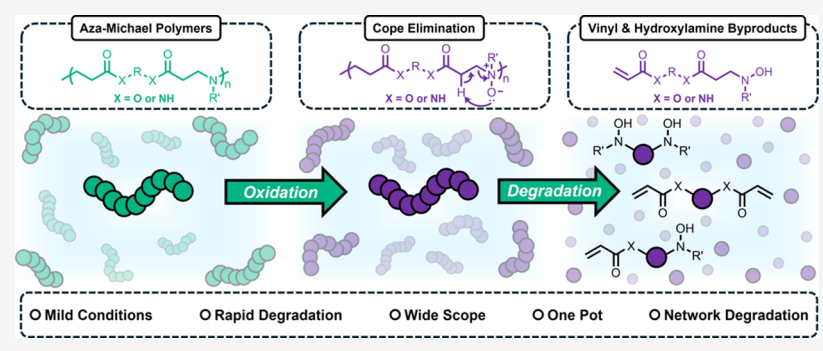


Cite This: *Macromolecules* 2024, 57, 7547–7555



ACCESS IIII Metr&Mosre

🖽 ArtiRœlceommendat i ons 🗊 Support thi froog mation



ABSTRACT: We report on a mild and efficient method to degrade poly(β -amino esters) (PBAEs) and poly(amido amines) (PAMAMs) via Cope elimination. Oxidation of backbone tertiary amines to N-oxides allowed for the spontaneous abstraction of acidic β ester/amide protons, resulting in subsequent chain cleavage. We show that quantitative PBAE degradation can be achieved within 15 min in several organic solvents by treatment with *meta*-chloroperbenzoic acid. Despite being a more robust substrate than the PBAEs, PAMAMs could also be fully degraded within 18 h via an aqueous degradation protocol with hydrogen peroxide. Mass spectrometry revealed similar degradation profiles for PBAEs and PAMAMs with vinyl, divinyl, and dihydroxylamine compounds being the major degradation byproducts. Finally, we demonstrate that Cope elimination-induced degradation under mild conditions can be extended to network polymers.

■ INTRODUCTION

To address challenges in plastic persistence, it is vital to develop highly tunable, degradable materials. $^{1-11}$ With this in mind, poly(β -amino esters) (PBAEs) and poly(amido amines) (PAMAMs) have garnered interest in biomedical and materials science due to their facile synthesis, controllable degradation lifetime, and biocompatibility. $^{12-15}$ These materials are typically prepared via bulk aza-Michael polymerization of diacrylates/acrylamides with primary amines. 16,17 This combinatorial approach allows for the preparation of materials libraries with highly customizable backbone and pendent group chemistries without the need for purification. $^{18-21}$ Because of this structural diversity and ease of synthesis, PBAEs and PAMAMs have been extensively investigated as degradable polymeric platforms in gene delivery, 18,20,22 bioimaging, 23,24 three-dimensional (3D) printing, 25,26 and dynamic covalent networks. $^{27-29}$

For most biological applications, PBAEs and PAMAMs are typically employed in their protonated form to impart polycationic character and maximize solubility for DNA polyplexing in gene therapy applications. ^{30–32} Despite this, PBAEs only exhibit significant rates of hydrolysis at elevated pH, thereby limiting degradability under the conditions in which the polymers are typically used. ³³ A recent report by

Letteri and co-workers found that a combination of localized pH change, 34,35 water organization, 36–38 dielectric change, 39 and/or amine-catalyzed hydrolysis 39–43 resulted in hydrolytic rate differentiation at higher pHs. 44 While this study focused on hydrophilic PBAEs, hydrophobic PBAEs have been found to primarily undergo hydrolysis via surface erosion, significantly reducing degradation kinetics. 25,45 Meanwhile, hydrophilic PAMAMs have been reported to undergo slow hydrolysis on a scale of months at high pH. 46,47 To address challenges with PBAE and PAMAM degradability, pH- and substrate-independent degradation techniques must be developed.

First developed in 1949, the Cope elimination promotes intramolecular elimination of an alkyl *N*-oxide to yield an alkene and a hydroxylamine. Typically, a tertiary amine is oxidized to yield a zwitterionic *N*-oxide, which can then abstract a β proton upon heating at 120–150 °C. The high

Received: May 24, 2024 Revised: July 3, 2024 Accepted: July 18, 2024 Published: July 31, 2024





Figure 1. Poly(β -amino ester)s (PBAEs) can be degraded by oxidizing the tertiary amine along the backbone to yield an N-oxide. Upon oxidation, the N-oxide will abstract a β proton, yielding two polymeric fragments terminated with hydroxylamine and acrylate. Further oxidation results in degradation to yield various vinyl- and hydroxylamine byproducts.

temperatures required have limited its utility in organic synthesis due to competition with side reactions, particularly with solvents typically employed for high-temperature reactions, such as DMF and DMSO. However, early work by Cram and Sahyun found that *N*-oxides can undergo spontaneous Cope elimination at room temperature in polar aprotic solvents, with rates of reaction 5 orders of magnitude greater in anhydrous DMSO compared to water. Kinetic studies suggested that this rate difference was attributable to hydrogen bonding of water to the oxyanion of the *N*-oxide, which increases the energy barrier for proton abstraction. Four decades later, Jorgensen and co-workers computationally demonstrated that the oxygen of the *N*-oxide could accept up to three hydrogen bonds, decreasing its basicity and thus the overall rate of elimination.

Localization of the tertiary amine near labile protons permits Cope elimination to be performed at significantly lower temperatures, allowing for substrates containing tertiary amines to be oxidized and immediately undergo elimination upon β proton abstraction. We reasoned PBAEs and PAMAMs represent ideal classes of model polymers to demonstrate the utility of the Cope elimination as a degradation mechanism, as these classes of polymers contain a tertiary amine along the backbone adjacent to relatively acidic β protons (p $K_{\rm a,ester}\approx 25$ and p $K_{\rm a,amide}\approx 30$). Since the N-oxide acts as an intramolecular base, we reasoned that the acidity of these β protons would promote facile degradation under mild conditions independent of substrate hydrophilicity. Therefore, we hypothesized that PBAEs and PAMAMs could undergo spontaneous degradation via a one-pot oxidation-elimination process to yield acrylic and

hydroxylamine byproducts (Figure 1). To this end, we prepared a library of PBAEs and PAMAMs via bulk aza-Michael polymerization of primary amines and diacrylates/acrylamides. Utilizing conditions optimized from a small-molecule study, we demonstrated that full degradation is achieved within 1 h across a variety of polar aprotic solvents. Upon identification of degradation products via ¹H NMR spectroscopy and mass spectrometry, a plausible degradation mechanism was developed. With these data, we further extended this protocol to more chemically robust PAMAMs, which underwent full degradation within 18 h. Finally, we demonstrated that a cross-linked PBAE network can undergo facile degradation under mild conditions.

■ RESULTS AND DISCUSSION

We first sought to develop a mild degradation protocol to determine whether PBAEs would be an appropriate substrate for Cope elimination. To this end, 2 equiv of methyl acrylate were reacted with 1 equiv of butylamine to yield a small-molecule β -amino ester aza-Michael adduct that would yield easily characterized degradation products (Figure S1). After 1 h of treating the aza-Michael adduct with *meta*-chloroperbenzoic acid (mCPBA) in DCM (Figure 2), an aliquot of the reaction solution was analyzed with 1 H NMR spectroscopy. Vinyl peaks were observed at 5.82, 6.12, and 6.37 ppm, corresponding to the vinyl protons of methyl acrylate. Additionally, a new peak appeared at 3.74 ppm, corresponding to the methyl ester. Further evidence of degradation was observed as a decrease in the normalized peak integration at

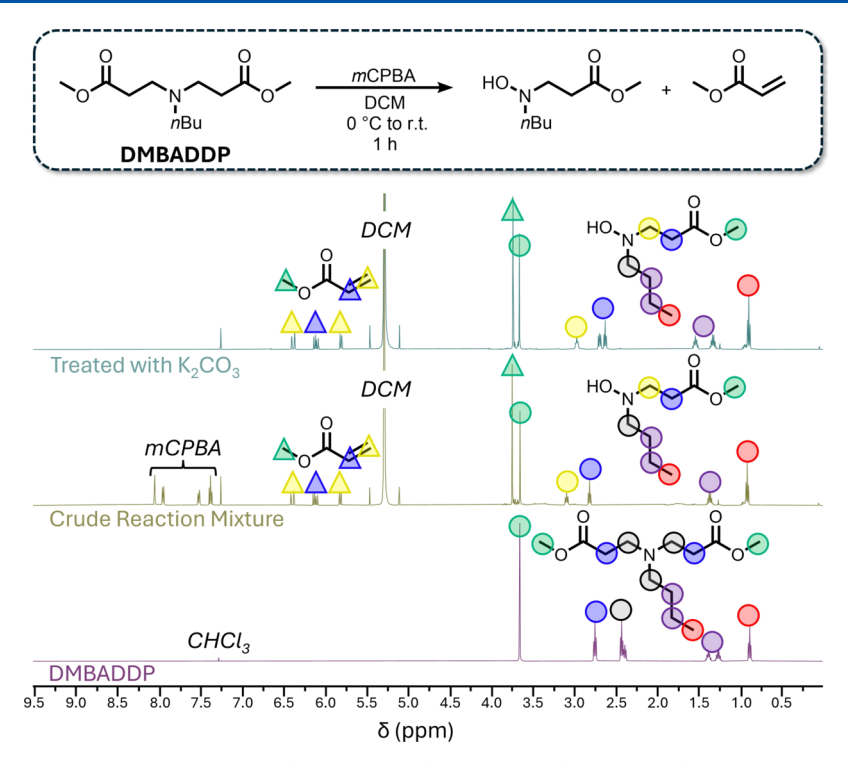


Figure 2. One-pot oxidation-elimination of dimethyl 3,3'-(butylazanediyl)dipropionate (DMBADDP) yields a hydroxylamine and methyl acrylate.

¹H NMR analysis of the crude reaction mixture (yellow spectrum) reveals the appearance of vinyl peaks (δ = 5.82, 6.12, and 6.37 ppm) and a methyl peak (δ = 3.74 ppm), corresponding to the generation of methyl acrylate. Quantitative removal of meta-chloroperbenzoic acid (mCPBA) and meta-chlorobenzoic acid (mCBA) could be achieved by treating the crude reaction mixture with potassium carbonate and filtering the precipitate off (green), as indicated by the complete disappearance of aromatic peaks (δ = 7.33–8.06 ppm).

Figure 3. Library of poly(β-amino ester)s (PBAEs) synthesized via bulk aza-Michael polymerization of primary amines (A = butylamine (BuNH₂) and B = benzylamine (BnNH₂)) and diacrylates (1 = diethylene glycol diacrylate (DEGDA), 2 = 1,6-hexanediol diacrylate (HDDA), 3 = neopentyl glycol diacrylate (NPDA), 4 = bisphenol A glycerolate diacrylate (BPADA), and 5 = 2-methyl-1,4-phenylene bis(4-(3-(acryloyloxy)propoxy)benzoate) (RM257)) at 90 °C for 20 h.

2.29–2.51 ppm from 6.0 to 4.0, indicative of a loss of two methylene protons. Removal of unreacted mCPBA and its byproduct (meta-chlorobenzoic acid, mCBA) was accomplished by treating the crude reaction solution with K_2 CO $_3$ for 15 min, resulting in deprotonation and subsequent precipitation of mCPBA and mCBA. These byproducts were then removed by filtration, after which 1 H NMR analysis of the filtrate revealed complete disappearance of the aromatic peaks (δ = 7.33–8.06 ppm) belonging to mCPBA and mCBA. Taken together, these data suggest that the Cope elimination could be an efficient route toward PBAE degradation with simple purification.

With good evidence that Cope elimination could be an effective form of degradation, we next synthesized a library of

PBAEs via bulk aza-Michael polymerization of primary amines and diacrylates. Specifically, we chose butylamine (A) and benzylamine (B) as monomers to install pendent groups to tune the glass transition temperature $(T_{\rm g})$ of the resulting polymers lower or higher, respectively. Five commercial diacrylates were selected to target properties such as hydrophilicity (1), ^{19,51,52} hydrophobicity (2 and 3), ^{53–55} shape-memory (4), ^{56,57} and liquid crystallinity (5). These diacrylates were chosen to exemplify the amenability of this strategy toward the degradation of materials that could be applicable in a number of fields. Further, we chose mostly hydrophobic comonomers to demonstrate highly efficient polymer degradation independent of substrate solvophobicity. As we utilized a combinatorial approach to prepare materials,

each polymer was named according to the combination of amine (A or B) and diacrylate (1–5) (Figure 3). All polymerizations were performed in bulk at 90 °C for 20 h, allowing the obtained polymers to be characterized without further purification (Figure 3). Generally, each PBAE was a viscous yellow oil, in addition to P4A and P4B, which were yellow, rubbery solids at room temperature. The PBAEs were then characterized via $^1\mathrm{H}$ NMR spectroscopy, size exclusion chromatography (SEC), and differential scanning calorimetry (DSC) to determine the structure, molecular weight, and T_g respectively.

Polymer structures were elucidated via 1H NMR spectroscopy using either the methyl ($\delta = 0.82-0.88$ ppm) of the butyl pendent group or the methylene ($\delta = 3.55-3.59$ ppm) of the benzyl pendent group as internal standards. PBAEs prepared from butylamine were consistently higher molecular weight than those prepared from benzylamine, as determined by SEC using multiangle light scattering (SEC-MALS) (Table 1).

Table 1. Summary of PBAEs and PAMAMs Prepared via Aza-Michael Polymerization

polymer	divinyl monomer	amino monomer	$M_{n,SEC}$ (g mol ⁻¹)	$T_{\rm g}$ (°C)
P1A	DEGDA	$BuNH_2$	5,320	-54
P1B	DEGDA	$BnNH_2$	4,010	-27
P2A	HDDA	$BuNH_2$	5,410	-75
P2B	HDDA	$BnNH_2$	2,640	-50
P3A	NPDA	$BuNH_2$	5,630	-54
P3B	NPDA	$BnNH_2$	5,070	-24
P4A	BPADA	$BuNH_2$	33,350	23
P4B	BPADA	$BnNH_2$	6,970	32
P5A	RM257	$BuNH_2$	9,210	-8
P5B	RM257	$BnNH_2$	3,910	2
P6A	MBA	$BuNH_2$	5,510	29
P6B	MBA	$BnNH_2$	4,150	50

Reyniers and co-workers have reported that the addition of primary amines to acrylates in aprotic solvents is faster than

subsequent addition of the newly formed secondary amine to a second acrylate.⁶¹ Key to this was finding that the proton transfer occurs mainly through assisted shuttling via an unreacted primary amine, which suggests that more basic amines should polymerize faster via aza-Michael polymerization. Therefore, this difference in molecular weight is likely due to lower steric hindrance and a slightly higher basicity of butylamine $(pK_a = 10.7)^{62}$ compared to benzylamine $(pK_a = 10.7)^{62}$ 9.5).63 Moreover, the effect of the pendent group was demonstrated via DSC, as P1A, P2A, and P3A exhibited T_g values around 25-30 °C lower than their benzyl pendent group analogs. Polymers with aromatic backbones displayed higher T_a values than those with aliphatic backbones, with P5A and PSB undergoing glass transitions at -7.6 and 2.3 °C, respectively. Incorporating H-bonding motifs within an aromatic backbone further increased the $T_{\rm g}$ values of P4A and P4B to 23 and 32 °C.

With a library of diverse PBAEs prepared, we next explored their degradation profiles. PBAEs were subjected to our previously developed Cope elimination conditions. As a model substrate, P3B was chosen for degradation studies as it exhibits the fewest number of signals in ¹H NMR spectroscopy, allowing for more convenient characterization. P3B was dissolved in DCM to yield a 10% w/v solution and subsequently treated with mCPBA (Figure 4A). Within 5 min, mCBA, the byproduct of oxidation, precipitated out of the solution, indicative of reaction progression. SEC analysis revealed that quantitative degradation was achieved within 15 min with no further change in elution volume after this point (Figure 4B). When these conditions were applied to the other PBAEs, similar degradation profiles were observed, with shifts to shorter elution times being achieved within 1 h (Figures S27–36). Furthermore, degradation was found to be amenable to several solvents, such as EtOAc, THF, 1,4-dioxane, and DMF, with full degradation noted within 1 h in all cases (Figure S37).

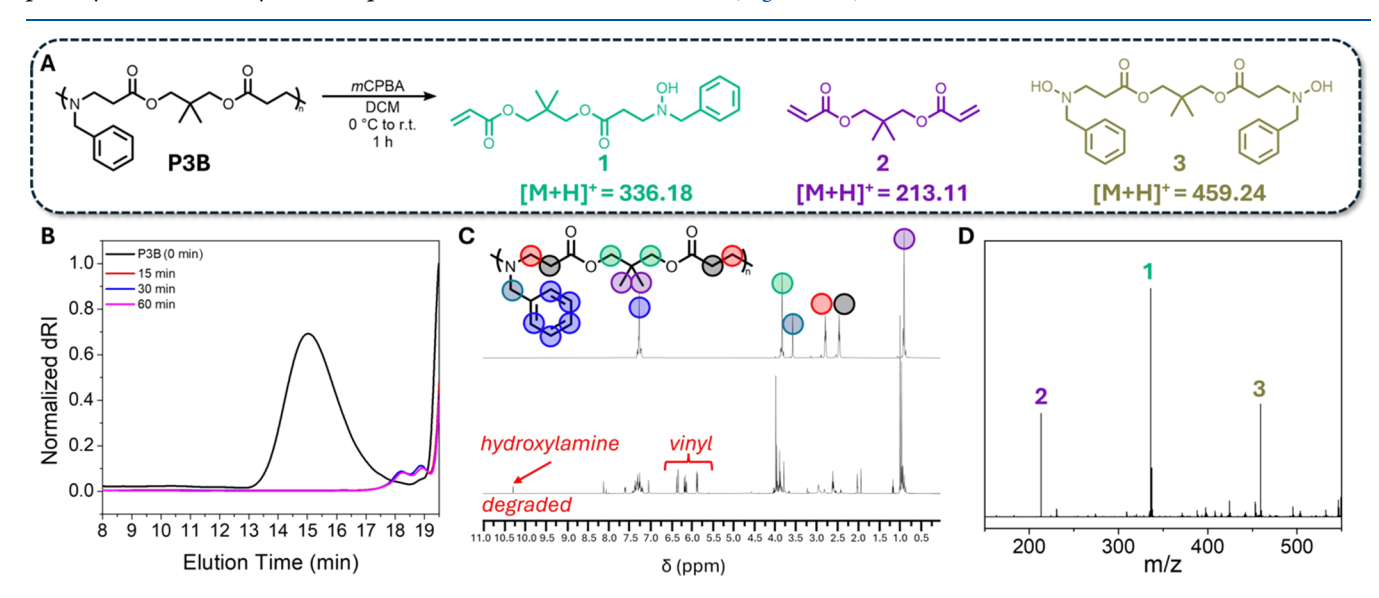


Figure 4. (A) P3B was degraded by treatment with a solution of mCPBA for 1 h to yield a mixture of three major degradation products. (B) Size exclusion chromatography (SEC) revealed quantitative degradation within 15 min with no change in retention volume afterward. (C) After degradation, peaks corresponding to hydroxylamine ($\delta = 10.4$ ppm) and vinyl (5.73–6.47 ppm) protons appeared, suggesting degradation through the Cope elimination. (D) Three major degradation products were identified via electrospray ionization mass spectrometry (ESI-MS) corresponding to an acrylate (1), diacrylate (2), and dihydroxylamine (3).

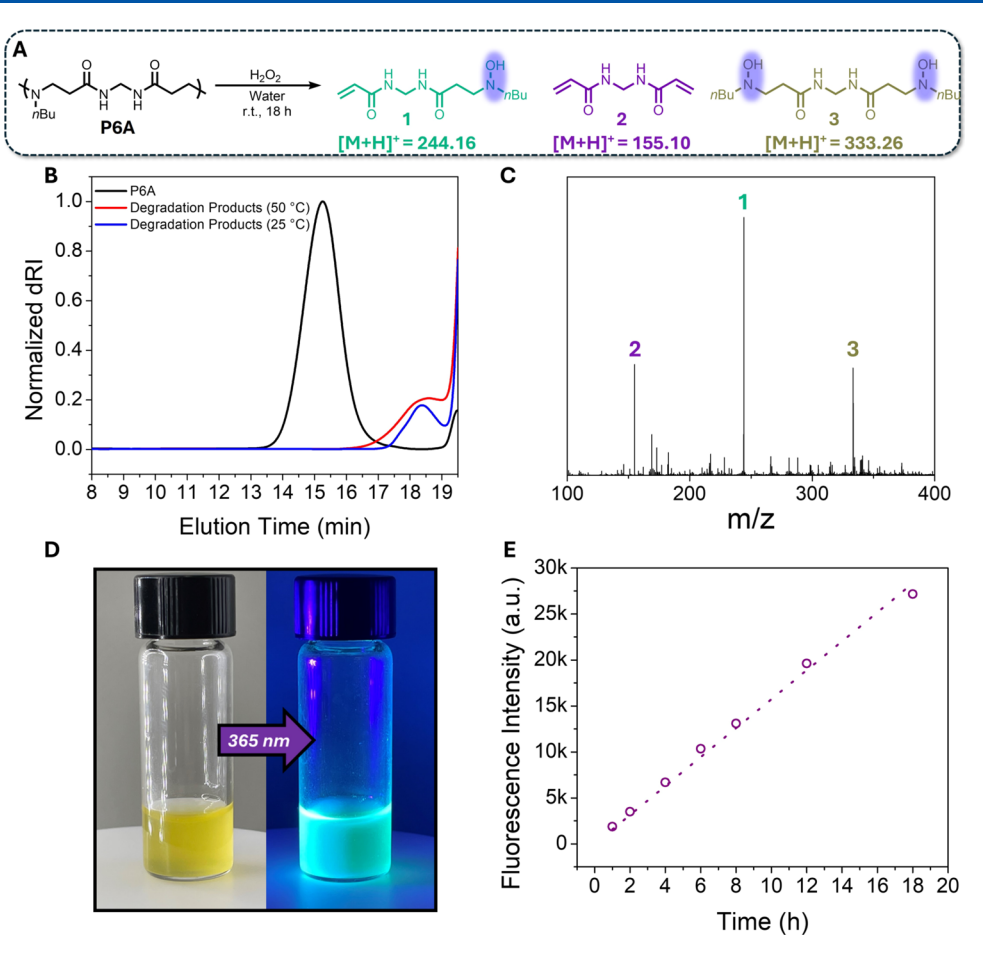


Figure 5. (A) As the PAMAMs were insoluble in most organic media, P6A was dissolved in water and treated with H_2O_2 to undergo Cope elimination. (B) Full degradation was observed after 18 h at both 50 and 24 °C. (C) ESI-MS revealed a similar degradation profile to the PBAEs, with three major products of the Cope elimination. (D) After degradation, the solution became bright yellow, with a bright blue fluorescence (λ_{max} = 459 nm) observed upon irradiation with UV light. This fluorescence was attributed to hydroxylamine degradation products (1 and 3). (E) Kinetic analysis of degradation via Cope elimination revealed a linear increase in fluorescence intensity (λ = 459 nm) over time.

To further demonstrate the versatility of oxidative degradation, we performed hydrolysis studies at pH = 9 on P1A (1 h) and P3B (6 h), hydrophilic, and hydrophobic PBAEs, respectively. As noted in previous studies, the hydrophilic PBAE underwent substantial degradation, whereas the hydrophobic PBAE exhibited minimal degradation. In comparison, both P1A and P3B demonstrated full degradation within 1 h upon oxidation in DCM (Figure S38). Furthermore, we developed an aqueous degradation protocol utilizing H₂O₂ to expand the solvent scope and serve as an appropriate comparison between hydrolysis and oxidation. Specifically, we found that P1A degraded fully within 1 h, analogous to the organic degradation protocol. Furthermore, P3B, despite being hydrophobic, underwent full degradation within 6 h, whereas little hydrolytic degradation was observed (Figure S39). These data indicate that Cope elimination can provide a more efficient means of degradation than hydrolysis. While SEC analysis provided evidence of degradation, we next sought to elucidate byproduct structures and mechanism via ¹H NMR spectroscopy and mass spectrometry.

 1 H NMR analysis revealed the disappearance of the methylene peaks (δ = 2.41 and 2.72 ppm) between the backbone amine and ester as well as the appearance of hydroxylamine (δ = 10.4 ppm) and vinyl (5.73–6.47 ppm) peaks (Figure 4C). The appearance of multiple peaks from 1.8

to 4.1 ppm suggests a mixture of degradation products. Electrospray ionization mass spectrometry (ESI-MS) was performed to gain further insight into the identity of the degradation fragments (Figure 4D). We observed three major products formed from the Cope elimination: an acrylate (1), a diacrylate (2), and a dihydroxylamine (3). These products suggest that upon oxidation of the tertiary amine, the N-oxide can abstract a proton from one of two possible methylenes. After the first elimination reaction, the polymer chain is cleaved into two fragments: one containing a terminal hydroxylamine and the other containing a terminal acrylate. Subsequent oxidation and elimination of the fragments can produce either an acrylate with a pendent hydroxylamine, the original diacrylate, or a dihydroxylamine (Figure S40). With a better understanding of the possible degradation products, we hypothesized that the Cope elimination could be further developed to degrade more robust polyamide substrates.^{64–67}

The aqueous degradation of PAMAMs has been reported to be extremely slow and inefficient. A recent study by Ranucci and Ferruti found that linear PAMAMs undergo faster degradation in high-pH solutions (pH > 7); however, most substrates exhibited less than 50% degradation after 90 days. Moreover, the authors demonstrated that the primary degradation mechanism of linear PAMAMs was a series of retro-aza-Michael additions, with minimal evidence of

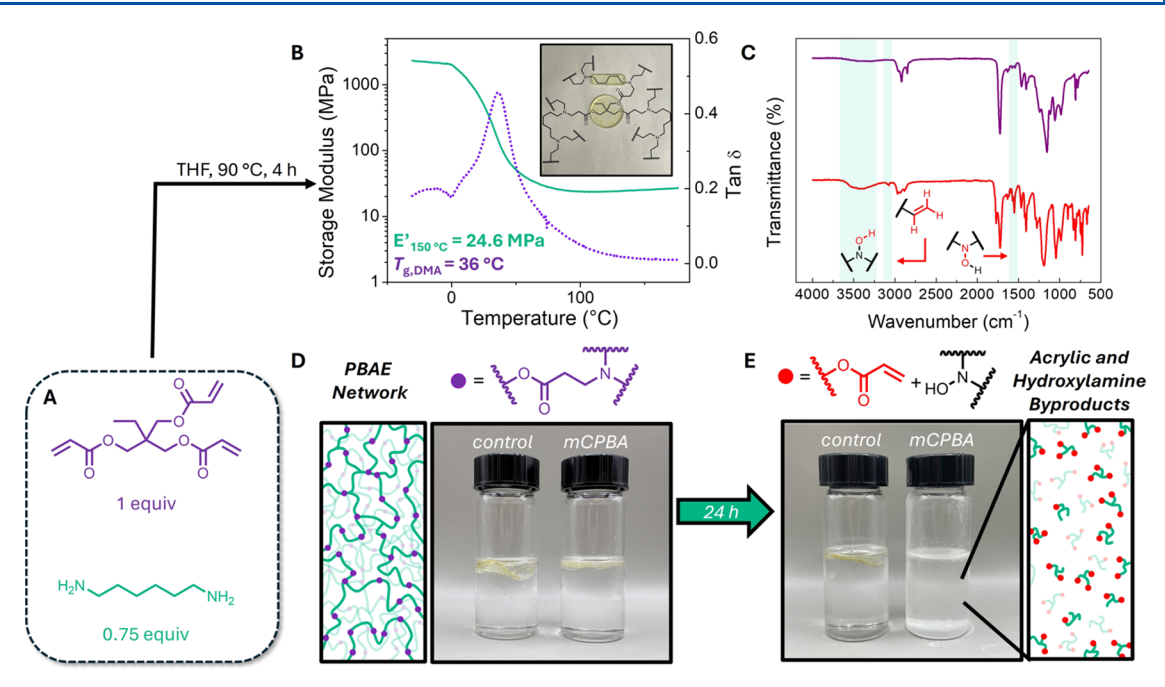


Figure 6. (A) PBAE covalent adaptable network (CAN) was prepared by solution-casting trimethylolpropane triacrylate and hexamethylene diamine. (B) Upon compression molding, a yellow transparent material was obtained. Dynamic mechanical analysis revealed a $T_{\rm g}$ of 36 °C (purple), as well as a rubbery plateau indicative of constant cross-link density. (C) Two CANs were added to a vial of DCM, with one vial being treated with mCPBA toward degradation. (D) FT-IR spectroscopy was performed on the CAN before (purple) and after (red) degradation. The appearance of peaks corresponding to hydroxylamine (1551 and 3160–3670 cm⁻¹) and vinyl (3100 cm⁻¹) products suggests degradation through Cope elimination. (E) After 24 h, the oxidized CAN had completely degraded, yielding a clear solution with insoluble mCBA precipitated at the bottom.

hydrolysis observed. With this in mind, we prepared two PAMAMs (P6A and P6B) via the aza-Michael polymerization of N,N'-methylene bis(acrylamide) (MBA) with BuNH₂ or BnNH₂. Since MBA is a high-melting-point solid ($T_{\rm m}$ = 182 °C), polymerization was performed at 80 °C for 18 h in a 2:1 MeOH/H2O solvent mixture. After polymerization, it was noted that P6B had precipitated, whereas the solution of P6A remained homogeneous. Nevertheless, both polymers were obtained as fine, white powders dissimilar to the viscous yellow PBAEs. SEC characterization revealed monomodal traces (Figures S22 and S24) with moderate molecular weights $(M_{n,P6A} = 5,500 \text{ g mol}^{-1} \text{ and } M_{n,P6B} = 4,150 \text{ g mol}^{-1})$. Similar to the case for the PBAE series, there was a 21 °C difference in T_g between P6A (29 °C) and P6B (50 °C). This increase in T_g compared to that of the PBAEs can be attributed to H-bonding and a shorter linker between the amide units. Because the polymers were only partially soluble in highly polar solvents, such as water and methanol, we elected to utilize an aqueous degradation protocol with H2O2 as described earlier.

With this in mind, we first attempted PAMAM degradation in water at 50 °C to ensure its solubility. To this end, P6A (10% w/w) was added to water and allowed to dissolve over an hour. Upon dissolution, hydrogen peroxide (2 equiv) was introduced and the reaction was allowed to proceed for 8 h. SEC analysis of the reaction solution revealed quantitative degradation of P6A (Figure 5B, red). As heating of peroxides can be dangerous, we next attempted to perform the degradation at room temperature. We reasoned that since the PAMAMs were minimally soluble, the solution would become homogeneous over time as the solubilized PAMAMs would degrade into water-soluble byproducts. Attempting to dissolve P6A and P6B in water at 10% w/v resulted in heterogeneous mixtures even after 3 h. Upon the addition of

hydrogen peroxide, however, both solutions became completely homogeneous within 15–20 min. Interestingly, after 1 h of dissolution, it was found that minimal degradation had occurred. We attribute this rate reduction to the H-bonding of both water and the amides to the newly formed *N*-oxide, which has been shown to retard the rate of elimination.²¹ Despite this, we found that quantitative degradation was still achieved within 18 h. Furthermore, it should be noted that **P6A** exhibited no degradation within 18 h when subjected to hydrolysis conditions (pH = 9), suggesting that oxidative degradation is the primary contributor to polymer degradation (Figure S43). Notably, the oxidative degradation solution became increasingly yellow as the reaction proceeded. Removal of the residual hydrogen peroxide and water via lyophilization yielded the degradation byproducts as a bright yellow powder.

Structural elucidation via ESI-MS confirmed that the degradation profiles of PAMAMs were similar to those of PBAEs, with three major peaks being attributed to an acrylamide, diacrylamide, and dihydroxylamine (Figure 5C). Comparing the absorbance of P6A before and after degradation, we found that P6A exhibited no absorbance from 270 to 750 nm. However, after degradation, a strong absorbance was observed from 270 to 425 nm (Figure S45). Moreover, fluorescence spectroscopy of the degradation products revealed a strong emission in the blue light region $(\lambda_{\text{max}} = 459 \text{ nm})$ when excited by ultraviolet (UV) light (365) nm) (Figure S46). As methylene bis(acrylamide) is a colorless solid, we rationalized that the color and fluorescence are likely from the hydroxylamine products. We reasoned that we could leverage the increase in the hydroxylamine fluorophore concentration over time to kinetically monitor the degradation process. Aliquots were taken periodically, and the fluorescence was monitored over time via fluorescence spectroscopy. As

hypothesized, the fluorescence increased over time (Figure S46), indicating an increase in hydroxylamine concentration. When the fluorescence at 459 nm was plotted against time, a linear relationship was observed (Figure SE), suggesting that fluorescence spectroscopy could be an effective means to monitor the reaction progress.

Finally, we explored the viability of this approach toward degrading polymeric networks. To this end, we prepared a covalent adaptable network (CAN) by solution-casting trimethylolpropane triacrylate and hexamethylene diamine.² The solvent was allowed to evaporate, and the film was cured at 90 °C for 4 h under a vacuum (Figure 6A). Thermogravimetric analysis revealed a degradation onset (T₉₅) at around 259 °C, affording a wide processing window (Figure S47). Upon compression molding at 180 °C, yellow optically transparent disks and bars were obtained. From DMA, the CAN exhibited a $T_{\rm g}$ of 36 °C as well as a rubbery plateau, indicative of constant cross-link density (Figure 6B). To demonstrate the applicability of the Cope elimination toward network degradation, two PBAE CAN disks were each added to a vial of DCM (Figure 6D). mCPBA was added to one vial, and the other was kept unoxidized as a control. After 24 h, the oxidized CAN had completely degraded, leaving a clear solution with insoluble mCBA sediment at the bottom. Conversely, the control maintained its structure over 24 h, indicating that degradation occurred after oxidation through Cope elimination. Fourier-transform infrared (FT-IR) spectroscopy of the CAN before and after degradation revealed three distinct peaks indicative of degradation through Cope elimination (Figure 5C). Specifically, it was found that an O-H peak (3160-3670 cm⁻¹) and N-O peak (1551 cm⁻¹) appeared (attributed to the hydroxylamine), while a C-H stretch peak appeared at 3100 cm⁻¹ (attributed to the vinyl C-H bond). From these data, we highlight that cross-linked networks containing β -amino esters can be effectively degraded under mild conditions via the Cope elimination.

CONCLUSIONS

While efficient degradation of PBAEs and PAMAMs is typically limited to hydrophilic substrates at a high pH, we showed that Cope elimination can be used as a versatile synthetic tool for degradation independent of hydrophilicity. We demonstrated this by preparing a library of PBAEs and PAMAMs across a range of material properties via aza-Michael polymerization. Utilizing a mild, organic degradation protocol with mCPBA as an oxidant, SEC revealed that all PBAEs could undergo full degradation within 1 h regardless of structure. Furthermore, PAMAMs were also found to be amenable to quantitative degradation through Cope elimination via an aqueous protocol with hydrogen peroxide. Similar degradation profiles were observed for both PBAEs and PAMAMs via ¹H NMR spectroscopy and ESI-MS. Degradation is likely to occur through the oxidation of backbone tertiary amines to N-oxides that undergo a spontaneous intramolecular β -proton abstraction. This yields two polymeric fragments bearing an acryloyl and hydroxylamino terminal end. Further degradation yields three main small-molecule products—an acryloyl, a bisacryloyl, and a bishydroxylamino product. As PBAEs and PAMAMs are primarily used as biomaterials, future studies will need to be performed to consider the role of biologically derived reactive oxygen species (e.g., superoxide, singlet oxygen, peroxynitrite) toward polymer oxidation and degradation. Furthermore, we foresee this strategy being amenable toward the

degradation of thiol-Michael-derived polymers, where thioethers can be oxidized to sulfoxides which can abstract acidic protons. While this report focuses on polymer degradation, we believe the Cope elimination bears great potential in polymer science as a synthetic tool for applications such as postpolymerization modification, sensing, and responsive materials.

ASSOCIATED CONTENT

Supporting Information

The Supporting Information is available free of charge at https://pubs.acs.org/doi/10.1021/acs.macromol.4c01186.

Materials and instrumentation; ¹H NMR spectra; SEC chromatographs; DSC thermograms; TGA thermogram; UV–vis and fluorescence spectra; summary of SEC and DSC data; and proposed degradation mechanism (PDF)

AUTHOR INFORMATION

Corresponding Author

Brent S. Sumerlin — George & Josephine Butler Polymer Research Laboratory, Center for Macromolecular Science & Engineering, Department of Chemistry, University of Florida, Gainesville, Florida 32611, United States; © orcid.org/ 0000-0001-5749-5444; Email: sumerlin@chem.ufl.edu

Authors

- Jared I. Bowman George & Josephine Butler Polymer Research Laboratory, Center for Macromolecular Science & Engineering, Department of Chemistry, University of Florida, Gainesville, Florida 32611, United States
- James B. Young George & Josephine Butler Polymer Research Laboratory, Center for Macromolecular Science & Engineering, Department of Chemistry, University of Florida, Gainesville, Florida 32611, United States
- Victoria L. Thompson George & Josephine Butler Polymer Research Laboratory, Center for Macromolecular Science & Engineering, Department of Chemistry, University of Florida, Gainesville, Florida 32611, United States
- Kevin A. Stewart George & Josephine Butler Polymer Research Laboratory, Center for Macromolecular Science & Engineering, Department of Chemistry, University of Florida, Gainesville, Florida 32611, United States
- Lily E. Diodati George & Josephine Butler Polymer Research Laboratory, Center for Macromolecular Science & Engineering, Department of Chemistry, University of Florida, Gainesville, Florida 32611, United States
- Kaden C. Stevens George & Josephine Butler Polymer Research Laboratory, Center for Macromolecular Science & Engineering, Department of Chemistry, University of Florida, Gainesville, Florida 32611, United States; orcid.org/ 0000-0002-5853-8765
- Cabell B. Eades George & Josephine Butler Polymer Research Laboratory, Center for Macromolecular Science & Engineering, Department of Chemistry, University of Florida, Gainesville, Florida 32611, United States; orcid.org/ 0000-0001-5216-8022

Complete contact information is available at: https://pubs.acs.org/10.1021/acs.macromol.4c01186

Notes

The authors declare no competing financial interest.

ACKNOWLEDGMENTS

This material was based on work supposed by the NSF (DMR-2404144) and the DoD through the ARO (W911NF-24-1-0050).

REFERENCES

- (1) Worch, J. C.; Dove, A. P. 100th Anniversary of Macromolecular Science Viewpoint: Toward Catalytic Chemical Recycling of Waste (and Future) Plastics. ACS Macro Lett. 2020, 9, 1494–1506.
- (2) Schneiderman, D. K.; Hillmyer, M. A. 50th Anniversary Perspective: There Is a Great Future in Sustainable Polymers. *Macromolecules* **2017**, *50*, 3733–3749.
- (3) Geyer, R.; Jambeck, J. R.; Law, K. L. Production, Use, and Fate of All Plastics Ever Made. *Sci. Adv.* **2017**, *3*, No. e1700782.
- (4) Trachsel, L.; Konar, D.; Hillman, J. D.; Davidson, C. L. G.; Sumerlin, B. S. Diversification of Acrylamide Polymers via Direct Transamidation of Unactivated Tertiary Amides. *J. Am. Chem. Soc.* **2024**, *146*, 1627–1634.
- (5) Young, J. B.; Bowman, J. I.; Eades, C. B.; Wong, A. J.; Sumerlin, B. S. Photoassisted Radical Depolymerization. *ACS Macro Lett.* **2022**, *11*, 1390–1395.
- (6) Jang, Y.-J.; Nguyen, S.; Hillmyer, M. A. Chemically Recyclable Linear and Branched Polyethylenes Synthesized from Stoichiometrically Self-Balanced Telechelic Polyethylenes. *J. Am. Chem. Soc.* **2024**, 146, 4771–4782.
- (7) Abel, B. A.; Snyder, R. L.; Coates, G. W. Chemically Recyclable Thermoplastics from Reversible-Deactivation Polymerization of Cyclic Acetals. *Science* **2021**, *373*, 783–789.
- (8) Arroyave, A.; Cui, S.; Lopez, J. C.; Kocen, A. L.; LaPointe, A. M.; Delferro, M.; Coates, G. W. Catalytic Chemical Recycling of Post-Consumer Polyethylene. *J. Am. Chem. Soc.* **2022**, *144*, 23280–23285.
- (9) Arrington, A. S.; Long, T. E. Influence of Carboxytelechelic Oligomer Molecular Weight on the Properties of Chain Extended Polyethylenes. *Polymer* **2022**, *259*, No. 125319.
- (10) Häußler, M.; Eck, M.; Rothauer, D.; Mecking, S. Closed-Loop Recycling of Polyethylene-like Materials. *Nature* **2021**, *590*, 423–427.
- (11) Wang, H. S.; Truong, N. P.; Pei, Z.; Coote, M. L.; Anastasaki, A. Reversing RAFT Polymerization: Near-Quantitative Monomer Generation Via a Catalyst-Free Depolymerization Approach. *J. Am. Chem. Soc.* **2022**, *144*, 4678–4684.
- (12) Wei, J.; Zhu, L.; Lu, Q.; Li, G.; Zhou, Y.; Yang, Y.; Zhang, L. Recent Progress and Applications of Poly(Beta Amino Esters)-Based Biomaterials. *J. Controlled Release* **2023**, *354*, 337–353.
- (13) Wang, X.; Zhang, Z.; Hadjichristidis, N. Poly(Amino Ester)s as an Emerging Synthetic Biodegradable Polymer Platform: Recent Developments and Future Trends. *Prog. Polym. Sci.* **2023**, 136, No. 101634
- (14) Karlsson, J.; Rhodes, K. R.; Green, J. J.; Tzeng, S. Y. Poly(Beta-Amino Ester)s as Gene Delivery Vehicles: Challenges and Opportunities. *Expert Opin. Drug Delivery* **2020**, *17*, 1395–1410.
- (15) Ferruti, P. Poly(Amidoamine)s: Past, Present, and Perspectives. J. Polym. Sci., Part A: Polym. Chem. 2013, 51, 2319–2353.
- (16) Eltoukhy, A. A.; Siegwart, D. J.; Alabi, C. A.; Rajan, J. S.; Langer, R.; Anderson, D. G. Effect of Molecular Weight of Amine End-Modified Poly(β -Amino Ester)s on Gene Delivery Efficiency and Toxicity. *Biomaterials* **2012**, *33*, 3594–3603.
- (17) Kuenen, M. K.; Cuomo, A. M.; Gray, V. P.; Letteri, R. A. Net Anionic Poly(β -Amino Ester)s: Synthesis, pH-Dependent Behavior, and Complexation with Cationic Cargo. *Polym. Chem.* **2023**, *14*, 421–431.
- (18) Akinc, A.; Anderson, D. G.; Lynn, D. M.; Langer, R. Synthesis of Poly(β -Amino Ester)s Optimized for Highly Effective Gene Delivery. *Bioconjugate Chem.* **2003**, *14*, 979–988.
- (19) Lynn, D. M.; Anderson, D. G.; Putnam, D.; Langer, R. Accelerated Discovery of Synthetic Transfection Vectors: Parallel Synthesis and Screening of a Degradable Polymer Library. *J. Am. Chem. Soc.* **2001**, *123*, 8155–8156.

- (20) Zugates, G. T.; Tedford, N. C.; Zumbuehl, A.; Jhunjhunwala, S.; Kang, C. S.; Griffith, L. G.; Lauffenburger, D. A.; Langer, R.; Anderson, D. G. Gene Delivery Properties of End-Modified Poly(β -Amino Ester)s. *Bioconjugate Chem.* **2007**, *18*, 1887–1896.
- (21) Sun, H.; Dobbins, D. J.; Dai, Y.; Kabb, C. P.; Wu, S.; Alfurhood, J. A.; Rinaldi, C.; Sumerlin, B. S. Radical Departure: Thermally-Triggered Degradation of Azo-Containing Poly(β -Thioester)s. *ACS Macro Lett.* **2016**, *5*, 688–693.
- (22) Kim, J.; Mondal, S. K.; Tzeng, S. Y.; Rui, Y.; Al-kharboosh, R.; Kozielski, K. K.; Bhargav, A. G.; Garcia, C. A.; Quiñones-Hinojosa, A.; Green, J. J. Poly(Ethylene Glycol)—Poly(Beta-Amino Ester)-Based Nanoparticles for Suicide Gene Therapy Enhance Brain Penetration and Extend Survival in a Preclinical Human Glioblastoma Orthotopic Xenograft Model. ACS Biomater. Sci. Eng. 2020, 6, 2943—2955.
- (23) Koo, H.; Lee, H.; Lee, S.; Min, K. H.; Kim, M. S.; Lee, D. S.; Choi, Y.; Kwon, I. C.; Kim, K.; Jeong, S. Y. In Vivo Tumor Diagnosis and Photodynamic Therapy via Tumoral pH-Responsive Polymeric Micelles. *Chem. Commun.* **2010**, *46*, 5668–5670.
- (24) Kim, J.; Shamul, J. G.; Shah, S. R.; Shin, A.; Lee, B. J.; Quinones-Hinojosa, A.; Green, J. J. Verteporfin-Loaded Poly-(Ethylene Glycol)-Poly(Beta-Amino Ester)-Poly(Ethylene Glycol) Triblock Micelles for Cancer Therapy. *Biomacromolecules* **2018**, *19*, 3361–3370.
- (25) Muralidharan, A.; McLeod, R. R.; Bryant, S. J. Hydrolytically Degradable Poly(β -Amino Ester) Resins with Tunable Degradation for 3D Printing by Projection Micro-Stereolithography. *Adv. Funct. Mater.* **2022**, 32, No. 2106509.
- (26) Hu, Y.; Tang, H.; Xu, N.; Kang, X.; Wu, W.; Shen, C.; Lin, J.; Bao, Y.; Jiang, X.; Luo, Z. Adhesive, Flexible, and Fast Degradable 3D-Printed Wound Dressings with a Simple Composition. *Adv. Healthcare Mater.* **2024**, *13*, No. 2302063.
- (27) Taplan, C.; Guerre, M.; Du Prez, F. E. Covalent Adaptable Networks Using β -Amino Esters as Thermally Reversible Building Blocks. *J. Am. Chem. Soc.* **2021**, *143*, 9140–9150.
- (28) Nguyen, L. T.; Portone, F.; Prez, F. E. D. β -Amino Amide Based Covalent Adaptable Networks with High Dimensional Stability. *Polym. Chem.* **2023**, *15*, 11–16.
- (29) Holloway, J. O.; Taplan, C.; Prez, F. E. D. Combining Vinylogous Urethane and β -Amino Ester Chemistry for Dynamic Material Design. *Polym. Chem.* **2022**, *13*, 2008–2018.
- (30) Wilson, D. R.; Suprenant, M. P.; Michel, J. H.; Wang, E. B.; Tzeng, S. Y.; Green, J. J. The Role of Assembly Parameters on Polyplex Poly(Beta-Amino Ester) Nanoparticle Transfections. *Biotechnol. Bioeng.* **2019**, *116*, 1220–1230.
- (31) Dastgerdi, N. K.; Gumus, N.; Bayraktutan, H.; Jackson, D.; Polra, K.; McKay, P. F.; Atyabi, F.; Dinarvand, R.; Shattock, R. J.; Martinez-Pomares, L.; Gurnani, P.; Alexander, C. Charge Neutralized Poly(β -Amino Ester) Polyplex Nanoparticles for Delivery of Self-Amplifying RNA. *Nanoscale Adv.* **2024**, *6*, 1409–1422.
- (32) Piao, J.-G.; Yan, J.-J.; Wang, M.-Z.; Wu, D.-C.; You, Y.-Z. A New Method to Cross-Link a Polyplex for Enhancing in Vivo Stability and Transfection Efficiency. *Biomater. Sci.* **2014**, *2*, 390–398.
- (33) Kuenen, M. K.; Mullin, J. A.; Letteri, R. A. Buffering Effects on the Solution Behavior and Hydrolytic Degradation of Poly(β -Amino Ester)s. *J. Polym. Sci.* **2021**, *59*, 2212–2221.
- (34) Murmiliuk, A.; Košovan, P.; Janata, M.; Procházka, K.; Uhlík, F.; Štěpánek, M. Local pH and Effective pK of a Polyelectrolyte Chain: Two Names for One Quantity? ACS Macro Lett. 2018, 7, 1243–1247.
- (35) Nová, L.; Uhlík, F.; Košovan, P. Local pH and Effective pKA of Weak Polyelectrolytes Insights from Computer Simulations. *Phys. Chem. Chem. Phys.* **2017**, *19*, 14376–14387.
- (36) Chen, S.; Wang, Z.-G. Using Implicit-Solvent Potentials to Extract Water Contributions to Enthalpy—Entropy Compensation in Biomolecular Associations. *J. Phys. Chem. B* **2023**, *127*, 6825–6832.
- (37) Shen, K.; Wang, Z.-G. Polyelectrolyte Chain Structure and Solution Phase Behavior. *Macromolecules* **2018**, *51*, 1706–1717.
- (38) Wang, Z.-G. Effects of Ion Solvation on the Miscibility of Binary Polymer Blends. J. Phys. Chem. B 2008, 112, 16205–16213.

- (39) van de Wetering, P.; Zuidam, N. J.; van Steenbergen, M. J.; van der Houwen, O. A. G. J.; Underberg, W. J. M.; Hennink, W. E. A Mechanistic Study of the Hydrolytic Stability of Poly(2-(Dimethylamino)Ethyl Methacrylate). *Macromolecules* 1998, 31, 8063–8068.
- (40) Ros, S.; Burke, N. A. D.; Stöver, H. D. H. Synthesis and Properties of Charge-Shifting Polycations: Poly[3-Aminopropylmethacrylamide-Co-2-(Dimethylamino)Ethyl Acrylate]. *Macromolecules* **2015**, *48*, 8958–8970.
- (41) Ros, S.; Wang, J.; Burke, N. A. D.; Stöver, H. D. H. A Mechanistic Study of the Hydrolysis of Poly[N,N-(Dimethylamino)-Ethyl Acrylates] as Charge-Shifting Polycations. *Macromolecules* **2020**, 53, 3514–3523.
- (42) Truong, N. P.; Jia, Z.; Burges, M.; McMillan, N. A. J.; Monteiro, M. J. Self-Catalyzed Degradation of Linear Cationic Poly(2-Dimethylaminoethyl Acrylate) in Water. *Biomacromolecules* **2011**, *12*, 1876–1882.
- (43) Bowman, J. I.; Eades, C. B.; Korpanty, J.; Garrison, J. B.; Scheutz, G. M.; Goodrich, S. L.; Gianneschi, N. C.; Sumerlin, B. S. Controlling Morphological Transitions of Polymeric Nanoparticles via Doubly Responsive Block Copolymers. *Macromolecules* **2023**, *56*, 3316–3323.
- (44) Kuenen, M. K.; Reilly, K. S.; Letteri, R. A. Elucidating the Effect of Amine Charge State on Poly(β -Amino Ester) Degradation Using Permanently Charged Analogs. *ACS Macro Lett.* **2023**, *12*, 1416–1422
- (45) Muralidharan, A.; Crespo-Cuevas, V.; Ferguson, V. L.; McLeod, R. R.; Bryant, S. J. Effects of Kinetic Chain Length on the Degradation of Poly(β -Amino Ester)-Based Networks and Use in 3D Printing by Projection Microstereolithography. *Biomacromolecules* **2022**, 23, 3272–3285.
- (46) Arioli, M.; Manfredi, A.; Alongi, J.; Ferruti, P.; Ranucci, E. Highlight on the Mechanism of Linear Polyamidoamine Degradation in Water. *Polymers* **2020**, *12*, No. 1376.
- (47) Ferruti, P.; Mauro, N.; Falciola, L.; Pifferi, V.; Bartoli, C.; Gazzarri, M.; Chiellini, F.; Ranucci, E. Amphoteric, Prevailingly Cationic L-Arginine Polymers of Poly(Amidoamino Acid) Structure: Synthesis, Acid/Base Properties and Preliminary Cytocompatibility and Cell-Permeating Characterizations. *Macromol. Biosci.* **2014**, *14*, 390–400.
- (48) Cope, A. C.; Foster, T. T.; Towle, P. H. Thermal Decomposition of Amine Oxides to Olefins and Dialkylhydroxylamines. *J. Am. Chem. Soc.* **1949**, *71*, 3929–3934.
- (49) Cram, D. J.; Sahyun, M. R. V. Room Temperature Wolff-Kishner Reduction and Cope Elimination Reactions. *J. Am. Chem. Soc.* **1962**, *84*, 1734–1735.
- (50) Acevedo, O.; Jorgensen, W. L. Cope Elimination: Elucidation of Solvent Effects from QM/MM Simulations. *J. Am. Chem. Soc.* **2006**, 128, 6141–6146.
- (51) McBath, R. A.; Shipp, D. A. Swelling and Degradation of Hydrogels Synthesized with Degradable Poly(β -Amino Ester) Crosslinkers. *Polym. Chem.* **2010**, *1*, 860–865.
- (52) Filipović, V. V.; Nedeljković, B. Đ. B.; Vukomanović, M.; Tomić, S. L. Biocompatible and Degradable Scaffolds Based on 2-Hydroxyethyl Methacrylate, Gelatin and Poly(Beta Amino Ester) Crosslinkers. *Polym. Test.* **2018**, *68*, 270–278.
- (53) Chan, M.; Schopf, E.; Sankaranarayanan, J.; Almutairi, A. Iron Oxide Nanoparticle-Based Magnetic Resonance Method to Monitor Release Kinetics from Polymeric Particles with High Resolution. *Anal. Chem.* **2012**, *84*, 7779–7784.
- (54) Love, D.; Kim, K.; Domaille, D. W.; Williams, O.; Stansbury, J.; Musgrave, C.; Bowman, C. Catalyst-Free, Aza-Michael Polymerization of Hydrazides: Polymerizability, Kinetics, and Mechanistic Origin of an α -Effect. *Polym. Chem.* **2019**, *10*, 5790–5804.
- (55) Zhang, Y.; Wang, R.; Hua, Y.; Baumgartner, R.; Cheng, J. Trigger-Responsive Poly(β -Amino Ester) Hydrogels. *ACS Macro Lett.* **2014**, *3*, 693–697.
- (56) Santiago, D.; De La Flor, S.; Ferrando, S.; Ramis, F.; Sangermano, X. Thermomechanical Properties and Shape-Memory

- Behavior of Bisphenol A Diacrylate-Based Shape-Memory Polymers. *Macromol. Chem. Phys.* **2016**, *217*, 39–50.
- (57) Ivaldi, C.; Laguzzi, E.; Ospina, V. M.; Antonioli, D.; Chiarcos, R.; Campo, F.; Cuminetti, N.; De Buck, J.; Laus, M. Exploiting β -Amino Ester Chemistry to Obtain Methacrylate-Based Covalent Adaptable Networks. *Polymer* **2024**, 293, No. 126636.
- (58) Yoon, H.-H.; Kim, D.-Y.; Jeong, K.-U.; Ahn, S. Surface Aligned Main-Chain Liquid Crystalline Elastomers: Tailored Properties by the Choice of Amine Chain Extenders. *Macromolecules* **2018**, *51*, 1141–1149.
- (59) Zou, W.; Lin, X.; Terentjev, E. M. Amine-Acrylate Liquid Single Crystal Elastomers Reinforced by Hydrogen Bonding. *Adv. Mater.* **2021**, 33, No. 2101955.
- (60) Ghimire, E.; Lindberg, C. A.; Jorgenson, T. D.; Chen, C.; De Pablo, J. J.; Dolinski, N. D.; Rowan, S. J. Robust and Programmable Liquid Crystal Elastomers through Catalytic Control of Dynamic Aza-Michael Reactions. *Macromolecules* **2024**, *57*, 682–690.
- (61) Desmet, G. B.; D'hooge, D. R.; Omurtag, P. S.; Espeel, P.; Marin, G. B.; Du Prez, F. E.; Reyniers, M.-F. Quantitative First-Principles Kinetic Modeling of the Aza-Michael Addition to Acrylates in Polar Aprotic Solvents. *J. Org. Chem.* **2016**, *81*, 12291–12302.
- (62) Rajan, V. K.; Muraleedharan, K. The pKa Values of Amine Based Solvents for CO2 Capture and Its Temperature Dependence—An Analysis by Density Functional Theory. *Int. J. Greenhouse Gas Control* **2017**, 58, 62–70.
- (63) Wiczling, P.; Kawczak, P.; Nasal, A.; Kaliszan, R. Simultaneous Determination of pKa and Lipophilicity by Gradient RP HPLC. *Anal. Chem.* **2006**, *78*, 239–249.
- (64) Park, J.; Easterling, C. P.; Armstrong, C. C.; Huber, D. L.; Bowman, J. I.; Sumerlin, B. S.; Winey, K. I.; Taylor, M. K. Nanoscale Layers of Precise Ion-Containing Polyamides with Lithiated Phenyl Sulfonate in the Polymer Backbone. *Polym. Chem.* **2022**, *13*, 5811–5819.
- (65) Adler-Abramovich, L.; Reches, M.; Sedman, V.; Allen, S.; Tendler, S.; Gazit, E. Thermal and Chemical Stability of Diphenylalanine Peptide Nanotubes: Implications for Nanotechnological Applications. *Langmuir* **2006**, *22*, 1313–1320.
- (66) Deshoulles, Q.; Le Gall, M.; Dreanno, C.; Arhant, M.; Priour, D.; Le Gac, P.-Y. Modelling Pure Polyamide 6 Hydrolysis: Influence of Water Content in the Amorphous Phase. *Polym. Degrad. Stab.* **2021**, *183*, No. 109435.
- (67) Ranganathan, P.; Chen, C.-W.; Rwei, S.-P.; Lee, Y.-H.; Ramaraj, S. K. Methods of Synthesis, Characterization and Biomedical Applications of Biodegradable Poly(Ester Amide)s- A Review. *Polym. Degrad. Stab.* **2020**, *181*, No. 109323.
- (68) Hu, B.; Lian, Z.; Zhou, Z.; Shi, L.; Yu, Z. Reactive Oxygen Species-Responsive Adaptable Self-Assembly of Peptides toward Advanced Biomaterials. *ACS Appl. Bio Mater.* **2020**, *3*, 5529–5551.
- (69) Nathan, C.; Cunningham-Bussel, A. Beyond Oxidative Stress: An Immunologist's Guide to Reactive Oxygen Species. *Nat. Rev. Immunol.* **2013**, *13*, 349–361.
- (70) Shafiq, M.; Chen, Y.; Hashim, R.; He, C.; Mo, X.; Zhou, X. Reactive Oxygen Species-Based Biomaterials for Regenerative Medicine and Tissue Engineering Applications. *Front. Bioeng. Biotechnol.* **2021**, *9*, No. 821288.
- (71) Zhou, J.; Fang, C.; Rong, C.; Luo, T.; Liu, J.; Zhang, K. Reactive Oxygen Species-Sensitive Materials: A Promising Strategy for Regulating Inflammation and Favoring Tissue Regeneration. *Smart Mater. Med.* **2023**, *4*, 427–446.